Products and Mechanism of Secondary Organic Aerosol Formation from Reactions of Linear Alkenes with NO_3 Radicals

Huiming Gong,[†] Aiko Matsunaga,[‡] and Paul J. Ziemann*[,§]

Air Pollution Research Center, University of California, Riverside, California 92521

Received: January 14, 2005; In Final Form: March 30, 2005

Secondary organic aerosol (SOA) formation from reactions of linear alkenes with NO_3 radicals was investigated in an environmental chamber using a thermal desorption particle beam mass spectrometer for particle analysis. A general chemical mechanism was developed to explain the formation of the observed SOA products. The major first-generation SOA products were hydroxynitrates, carbonylnitrates, nitrooxy peroxynitrates, dihydroxynitrates, and dihydroxy peroxynitrates. The major second-generation SOA products were hydroxy and oxo dinitrooxytetrahydrofurans, which have not been observed previously. The latter compounds were formed by a series of reactions in which δ-hydroxycarbonyls isomerize to cyclic hemiacetals, which then dehydrate to form substituted dihydrofurans (unsaturated compounds) that rapidly react with NO_3 radicals to form very low volatility products. For the ~1 ppmv alkene concentrations used here, aerosol formed only for alkenes C_7 or larger. SOA formed from C_7-C_9 alkenes consisted only of second-generation products, whereas for larger alkenes first-generation products were also present and contributions increased with increasing carbon number apparently due to the formation of lower volatility products. The estimated mass fractions of first- and second-generation products were approximately 50:50, 30:70, 10:90, and 0:100, for 1-tetradecene, 1-dodecene, 1-decene, and 1-octene SOA, respectively. This study shows that δ-hydroxycarbonyls play a key role in the formation of SOA in alkene−NO_3 reactions and are likely to be important in other systems because δ-hydroxycarbonyls can also be formed from reactions of OH radicals and O_3 with hydrocarbons.

Introduction

Organic particles are emitted directly into the atmosphere as products of incomplete combustion and are also formed by gas-to-particle conversion of volatile organic compounds (VOCs) emitted from anthropogenic and biogenic sources.[1] In the latter process, VOCs are oxidized to less volatile compounds that condense to form secondary organic aerosol (SOA). The major atmospheric reactions of VOCs are those involving OH and NO_3 radicals and O_3.[2] Reactions with OH radicals occur almost exclusively during the day, reactions with NO_3 radicals occur primarily at night, and reactions with O_3 occur during the day and at night. Most studies of SOA chemistry have focused on reactions of OH radicals with aromatics[3] and alkenes[4] and on reactions of O_3 with alkenes.[5,6] Little is known about the chemistry of SOA formation from NO_3 radical reactions.

Nitrate radicals are formed in the atmosphere by the reaction of NO_2 with O_3. Concentrations are maintained at very low levels during the day by photolysis[7] and by reaction with NO but increase near sunset and at night such that reactions with NO_3 radicals can become an important sink for organic compounds including unsaturated hydrocarbons, phenols, aldehydes, and dimethyl sulfide.[8,9] For example, recent field studies in two major urban areas have demonstrated that NO_3 radicals can contribute significantly to the oxidation of some VOCs.[10,11] It has also been suggested that reactions of VOCs with NO_3 radicals may be important in indoor air chemistry.[12] Although the kinetics, mechanisms, and gas-phase products of alkene−NO_3 reactions have been the subject of a relatively large number of laboratory studies (for reviews see refs 13 and 14), investigations of SOA formation are limited to a few measurements of aerosol yields.[15−18] Nonetheless, these studies show that the reactions can be efficient aerosol sources, as indicated by SOA yields approaching unity for some monoterpenes.[16]

In this study, the chemistry of SOA formation from reactions of NO_3 radicals with a suite of linear alkenes was investigated using a thermal desorption particle beam mass spectrometer (TDPBMS) for on-line aerosol analysis.[19,20] This instrument makes it possible to identify low-volatility multifunctional organic nitrates that have not been observed previously because of the inability of off-line methods (e.g., gas chromatography) to analyze these labile compounds. The compounds investigated included simple linear alkenes with double bonds in either terminal or internal locations. In the atmosphere, those with internal double bonds have lifetimes (calculated using rate constants from ref 14 and background oxidant concentrations from ref 21) with respect to reaction with NO_3 radicals of ~3 h, which is comparable to reactions with O_3 and OH radicals. Terminal alkenes react with NO_3 radicals (and O_3) much more slowly, so their atmospheric lifetime is determined by reaction with OH radicals. Although the emissions of linear alkenes large enough to form condensable products are probably too small to contribute significantly to atmospheric SOA formation, these compounds provide very useful models for the more abundant and complex monoterpenes. Because the present study represents the beginning of a larger investigation into the chemistry of SOA formation from alkene−NO_3 reactions, linear alkenes were

* Corresponding author. Phone: (951) 827-5127. Fax: (951) 827-5004. E-mail: paul.ziemann@ucr.edu.
[†] Also in the Environmental Toxicology Graduate Program.
[‡] Also in the Department of Chemistry.
[§] Also in the Department of Environmental Sciences, Department of Chemistry, and Environmental Toxicology Graduate Program.

10.1021/jp058024l CCC: $30.25
Published on Web 04/26/2005

selected to simplify the chemistry while still providing insight into the effects of molecular structure on the pathways that lead to aerosol products.

Experimental Section

Materials. The alkenes 1-hexene (99%), 1-heptene (99%), 1-octene (98%), 1-decene (94%), 1-dodecene (95%), and 1-tetradecene (92%) were obtained from Sigma-Aldrich, and 3,5,5-trimethyl-1-hexene (99%), 2-methyl-1-octene, and 7-tetradecene were obtained from ChemSampCo. All chemicals were used without further purification.

Environmental Chamber Technique. Reactions of alkenes with NO_3 radicals were performed in the dark in a ~7000 L PTFE environmental chamber at room temperature (~23 °C) and pressure (~96 kPa). The chamber was flushed overnight and filled with clean, dry air (<5 ppbv hydrocarbons, <0.1% RH) from an Aadco pure air generator. A measured amount of alkene was evaporated from a glass bulb using gentle heating and flushed into the chamber in a clean air stream. Nitrate radicals were added in the form of N_2O_5, which thermally dissociates into NO_3 and NO_2. N_2O_5 was synthesized according to the procedure of Atkinson et al.[22] and kept frozen in liquid N_2 on a glass vacuum rack until needed. When used, N_2O_5 was warmed and evaporated into an evacuated, calibrated 2.0 L bulb until an appropriate pressure was reached. The bulb was then flushed into the chamber using clean air. During these additions, a fan in the chamber was run to mix the reactants. Particles formed by homogeneous nucleation, typically within 1 min of adding N_2O_5 and increased from background concentrations of ~10 cm^{-3} to a peak of ~10^4−10^6 cm^{-3} a few minutes later. Average particle diameters were ~0.2−0.4 μm.

The initial concentration of alkene in the chamber was 1 ppmv. The amount of N_2O_5 added to the bulb (~0.34 kPa) was intended to also achieve this concentration. Some N_2O_5, however, was lost to the walls of the vacuum rack, glass bulb, and chamber. From the amount of reacted alkene measured in a few experiments, N_2O_5 losses were apparently <20%. At an initial N_2O_5 concentration of 1 ppmv, the equilibrium concentrations of NO_3 and NO_2 are 37 ppbv (calculated using an equilibrium constant of 2.9×10^{-11} cm^3 $molecule^{-1}$ [23]). As the alkene−NO_3 reaction proceeds, [NO_3] decreases due to reaction and to the shift in equilibrium as [N_2O_5] decreases and [NO_2] increases. The amount of alkene reacted at any time depends on the rate constant, which in turn depends on the structure of the molecule. For the compounds investigated here, the rate constants[14] are approximately 1×10^{-14} (terminal alkenes) and 3.6×10^{-13} (2-methyl-1-octene, 7-tetradecene) cm^3 $molecule^{-1}$ s^{-1}. Using the appropriate second-order kinetics expression and assuming no wall losses of N_2O_5, the amounts of alkene reacted in 1 h are calculated to be ~70% and ~98% for these two classes of compounds, respectively.

Particle Mass Spectrometric Analysis. The TDPBMS was used to analyze particle composition in real-time[19] and by temperature-programmed thermal desorption.[20] Aerosol is sampled from the chamber through stainless steel tubing and enters the TDPBMS through a 0.1 mm critical orifice that reduces the pressure from atmosphere to ~300 Pa. Particles are focused in an aerodynamic lens[24,25] and the resulting beam passes through a nozzle and two flat-plate skimmers before entering the detection chamber. In the detection chamber (~10^{-5} Pa), particles impact in a V-shaped notch in the tip of a copper vaporizer rod that for real-time analysis is resistively heated to ~165 °C. Particles are completely vaporized upon impact and vapor diffuses into an ABB Extrel MEXM 500 quadrupole mass spectrometer where molecules are ionized by electrons, mass-filtered, and detected using a conversion dynode/pulse counting detector. For TPTD analysis, the vaporizer rod was cooled to −30 °C, and particles were collected for ~15 min. The rod was allowed to warm to −5 °C and was then heated to ~90−120 °C using a computer controlled linear temperature ramp of 2 °C min^{-1}. Compounds desorb from the vaporizer according to their vapor pressures, allowing separation of components for mass spectral analysis. The mass spectrometer was typically scanned from m/z 10−400 in ~30 s. Although slightly better resolution might be obtained with a slower ramp, radiative heating by the ionizer sets a minimum heating rate of ~1−2 °C min^{-1}. This effect could be reduced with active cooling during ramping, but it would then be much more difficult to produce the exceptionally linear ramp we currently achieve and also lengthen the analysis time.

Aerosol Yield Measurements. In a few experiments, the aerosol yield [aerosol mass formed (μg m^{-3})/VOC mass reacted (μg m^{-3})][26] was determined from measurements of aerosol mass and reacted alkene concentrations.

The amount of alkene consumed was determined from the alkene concentrations measured before and after reaction using gas chromatography. For these measurements, 100 cm^3 of air was sampled onto solid Tenax TA adsorbent and analyzed immediately using a Hewlett-Packard (HP) 6890 GC system equipped with an HP-1701 fused-silica capillary column (30 m × 0.53 mm with a 1.0 μm film thickness) and a flame ionization detector (FID). The Tenax TA samples were placed in a split/splitless inlet that was run in the splitless mode. The inlet was initially at room temperature, and then ramped to 250 °C at a rate of ~23 °C min^{-1} after inserting the tube. The FID transfer line was maintained at 280 °C. The FID response was compared with standard calibrations to determine alkene concentrations.

The aerosol mass formed in a reaction was measured using a scanning mobility particle sizer (SMPS).[27] The SMPS consisted of a ^{210}Po bipolar charger, a long differential mobility analyzer similar in design to the TSI model 3934, a TSI Model 3010 Condensation Particle Counter, and a scanning/inversion program developed by the McMurry group at the University of Minnesota for use with Labview software.[28] The SMPS was operated at aerosol and sheath air flows of approximately 0.5 and 2.5 L min^{-1}, respectively, which provide a resolution of ~20% in particle size measurements. The software output includes the particle size distribution, number concentration, and volume concentration, the latter of which can be converted to a particle mass concentration by multiplying by the particle density. The density was assumed to be 1 g cm^{-3}.

Results and Discussion

Reaction Mechanism. *First-Generation Products.* On the basis of previous studies of the gas-phase products of the reactions of alkenes with NO_3 radicals,[29−34] the reaction of NO_3 radicals with a linear alkene [designated here as $R_X(CH_2)_3CH{=}CHR_Y$, where R_X and R_Y are alkyl groups] can potentially form first-generation products **1**−**16** by the mechanism shown in Figure 1. The reaction is initiated by the addition of NO_3 to the carbon−carbon double bond, with H-atom abstraction being negligible. Addition occurs predominantly at the less-substituted carbon atom due to the enhanced stability imparted to the radical site by the electron-donating alkyl group. For terminal alkenes, this means NO_3 adds primarily at the end of the molecule. The resulting nitrooxyalkyl radical reacts solely with O_2 to form a nitrooxyalkylperoxy radical. This radical can react with NO_2 to form a nitrooxyalkyl peroxynitrate [**1**], which is thermally

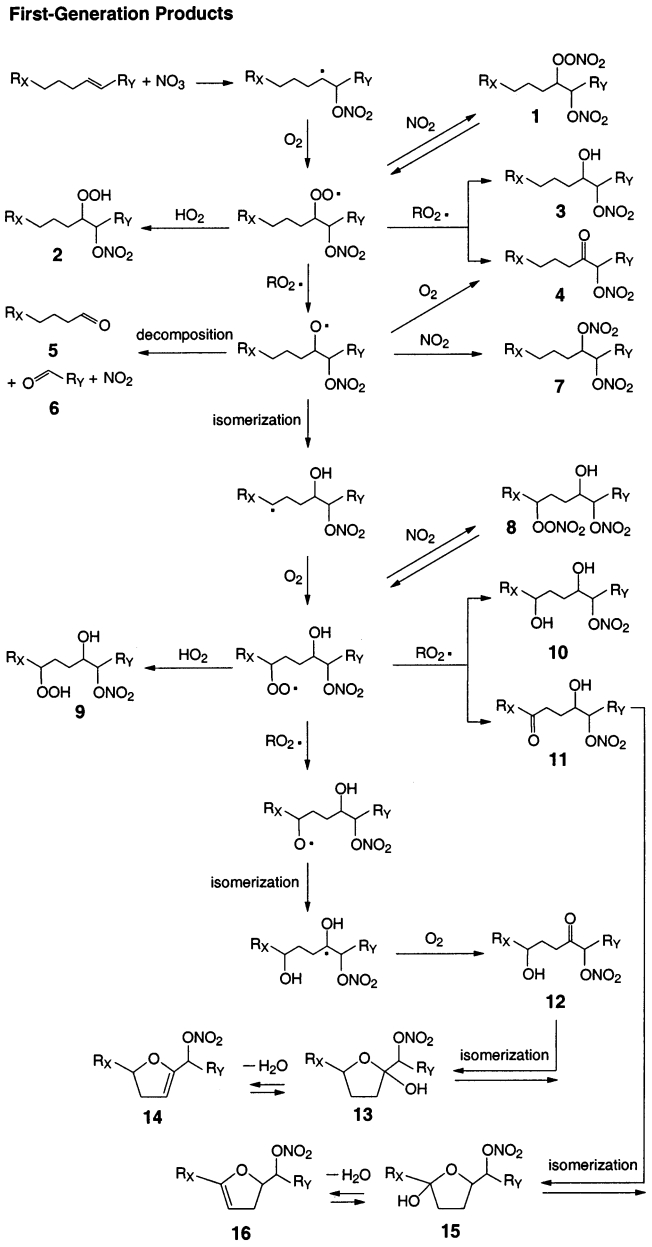

Figure 1. Proposed mechanism for forming first-generation products in reactions of linear alkenes with NO_3 radicals.

unstable and therefore acts as a temporary reservoir for the nitrooxyalkylperoxy radical. The nitrooxyalkylperoxy radical can also react with HO_2 to form a hydroperoxynitrate [**2**] or with other organic peroxy radicals ($RO_2^{\bullet}$) to form a hydroxynitrate [**3**], carbonylnitrate [**4**], or nitrooxyalkoxy radical. The nitrooxyalkoxy radical can decompose to aldehydes [**5**, **6**], isomerize through a 1,5 H-atom shift to a nitrooxyhydroxyalkyl radical, react with O_2 to form compound **4**, or react with NO_2 to form an alkyl dinitrate [**7**]. The nitrooxyhydroxyalkyl radical can subsequently undergo reactions similar to the nitrooxyalkyl radical to form products **8**−**12**.

Isomerization of δ-Hydroxycarbonyls: A Gateway to Second-Generation Reaction Products. The first-generation reaction products **1**−**12** are saturated compounds that react too slowly with NO_3 radicals for further reactions to occur. Recently, however, it has been shown that *δ*-hydroxycarbonyls (i.e., compounds in which CHOH and C═O groups are separated by two carbon atoms) similar to compounds **11** and **12** exist in the gas phase in equilibrium with a cyclic hemiacetal isomer, which in turn is in equilibrium with a substituted dihydrofuran formed by dehydration.[35,36] The equilibria shift in the direction of the substituted dihydrofuran with decreasing relative humidity (RH). For 5-hydroxy-2-pentanone (the only commercially available *δ*-hydroxycarbonyl), the lifetime for conversion to 4,5-dihydro-2-methylfuran is ∼1.1 h at RH ≪1%.[36] More recent studies on *δ*-hydroxycarbonyls created in chamber reactions have shown that as the carbon number of the *δ*-hydroxycarbonyl increases the equilibria shift toward the substituted dihydrofuran, with dehydration occurring as quickly as a few minutes or less.[37−39]

For compounds **11** and **12**, isomerization leads to cyclic hemiacetals **13** and **15**, which then lose water to form substituted dihydrofurans **14** and **16**, respectively. As shown below, formation of substituted dihydrofurans and their subsequent reactions with NO_3 radicals provides an important pathway to second-generation products of lower volatility and greater aerosol forming potential.

Second-Generation Products. It has been shown that the reaction of NO_3 radicals with 4,5-dihydro-2-methylfuran is orders of magnitude faster than with alkenes.[36] The substituted dihydrofuran compounds **14** and **16** therefore react rapidly with NO_3 radicals to form second-generation products. The proposed mechanism is shown in Figure 2 and is essentially the same as that shown in Figure 1 for alkenes (no reactions of nitrooxyalkoxy radicals with NO_2 are shown for reasons explained below, and an additional decomposition reaction leads to nitrooxycarbonyl esters [**21**, **29**]). The potential second-generation products of the reactions of compounds **14** and **16** are substituted tetrahydrofurans including nitroperoxy [**17**, **18**, **25**, **26**], hydroperoxy [**19**, **20**, **27**, **28**], hydroxy [**22**, **23**, **30**, **31**], and oxo [**24**, **32**] dinitrooxytetrahydrofurans.

Mass Spectral Analysis of Aerosol Products. The major challenge in using TDPBMS mass spectra to identify reaction products is that mass spectral standards are only available for the aldehyde products (**5** and **6**) formed by the mechanisms shown in Figures 1 and 2. The mass spectra of other potential products are not present in libraries nor are the compounds commercially available. The approach taken here was to use mass spectra of compounds with related structures, well-known electron ionization (EI) fragmentation pathways,[40] and TPTD profiles to determine which products of the proposed mechanisms appear to be present.

1-Tetradecene. The real-time mass spectrum obtained for the reaction of 1-tetradecene [$CH_3(CH_2)_{11}CH{=}CH_2$] with NO_3 radicals is shown in Figure 3. Significant high-mass peaks are present at *m*/*z* 333, 288, 286, 272, 258, 227, 211, 199, and 197. The TPTD desorption profiles for these and other selected *m*/*z* values are shown in Figure 4. For any single compound, the profiles of all *m*/*z* values that are present in its mass spectrum will exhibit maxima at the same temperature. A maximum in a desorption profile is therefore indicative of a single compound or a group of compounds having very similar vapor pressures. Although the TPTD technique was not able to completely separate the components of this mixture to obtain mass spectra of single compounds, by comparing profiles of different *m*/*z* values, it was possible to identify 6 compounds (or groups of compounds), corresponding to maxima at 30, 39, 48, 87, 92, and 96 °C.

The compound(s) responsible for each maximum was assigned by comparing potential reaction products, measured volatilities (as indicated by desorption temperatures), and major mass spectral peaks. For 1-tetradecene, $R_X = CH_3(CH_2)_8$ and $R_Y = H$ in the reaction schemes shown in Figures 1 and 2. The

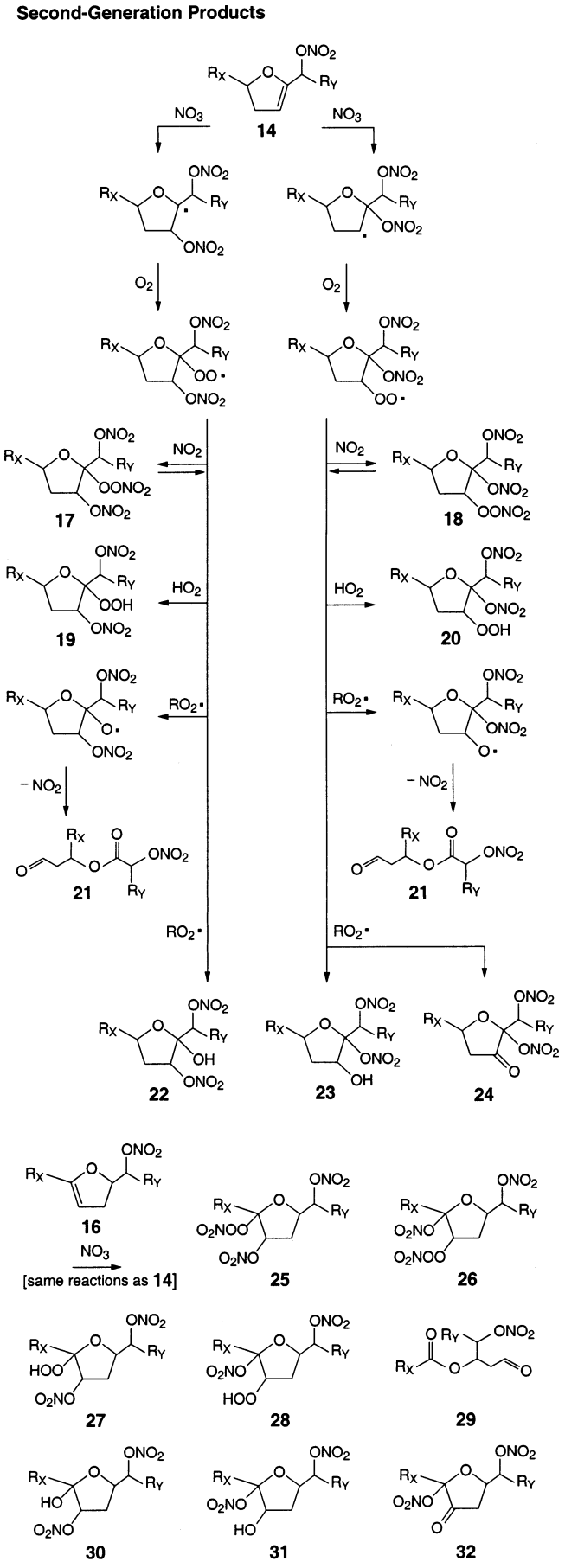

Figure 2. Proposed mechanism for forming second-generation products in reactions of linear alkenes with NO_3 radicals.

proposed aerosol products are shown in Figure 5 along with proposed pathways for creating the characteristic ions used for compound identification. The pathways are consistent with well-established electron ionization (EI) fragmentation mechanisms.[40] All the major mass spectral peaks associated with TPTD maxima can be assigned to stable ions generated from the proposed reaction products by loss of the molecular species H_2O, NO_2, HNO_2, NO_3, HNO_3, HCHO, $CH_2{=}CH_2$, and CO, and OH and alkyl radicals. The systematic procedure used to assign the products is described in detail below.

As a starting point, we note that compounds equivalent to **1**−**7** have been observed among the major gas-phase products of alkene−NO_3 reactions.[13,14,21] Whether or not these compounds are found in the aerosol analyzed here depends on the reaction conditions and the alkene carbon number, because products must have sufficiently low vapor pressures to partition into particles.

As shown in Figures 1 and 2, because the reaction of unsaturated compounds with NO_3 radicals is initiated by addition of NO_3 to the double bond, most of the products are expected to be nitrates with the exception of a few decomposition products. In EI mass spectra of organic nitrates, such as those shown in Figure 1S (Supporting Information) for alkyl nitrate standards, *m*/*z* 46 is a characteristic mass fragment due to NO_2^+. The TPTD profile of *m*/*z* 46 for aerosol formed from the 1-tetradecene reaction is shown in Figure 4A along with those for *m*/*z* 81, 83, and 85. The latter three ions are associated with many different products, and their profiles span the entire range of temperatures over which aerosol products desorb. The overlap of the desorption profiles of these peaks (as well as all others) with *m*/*z* 46 suggests that all the aerosol compounds are nitrates. Nonetheless, as we begin our analysis we will not assume this is the case. It is also important to note that many of the small mass fragments (e.g., *m*/*z* 46, 76, 81, 83, 85) have desorption profiles with maxima at temperatures other than those labeled in Figure 4. The reason for this is that these ions are associated with multiple compounds that are not completely separated by TPTD analysis. The low-mass *m*/*z* profiles therefore represent contributions from multiple products. In most cases, they exhibit maxima approximately midway between those of the labeled compound(s). High-mass fragments are more often characteristic of a single compound or isomers and are therefore more useful for identification.

We begin by determining whether any of the compounds **1**−**7** are present among the most volatile aerosol products, because their counterparts have been identified as gas-phase products in other alkene−NO_3 reactions. Beginning with the compound(s) that desorbs at 30 °C, we note that the highest *m*/*z* value that exhibits a maximum at this temperature is 199 (Figure 4B). This cannot be compound **5** (tridecanal) or **6** (formaldehyde), because our previous studies of 1-tetradecene ozonolysis[6] have shown that tridecanal (the least volatile of these) is too volatile to form particles under these conditions. Furthermore, the molecular weight of tridecanal is only198. Compound **7** is eliminated from consideration because dinitrate formation through reactions of alkoxy radicals with NO_2 should be negligible under the conditions of these experiments. For example, using a rate constant ratio of 4×10^3 for the reaction of alkoxy radicals with NO_2 relative to O_2[13] and the maximum value of $[NO_2]/[O_2] = 5 \times 10^{-6}$ in our experiments indicates that less than 2% of the nitrooxyalkoxy radicals react with NO_2. Isomerization and decomposition reactions will reduce this percentage further. Compound **2** is ruled out because in previous studies we observed that the mass spectra of hydroperoxides

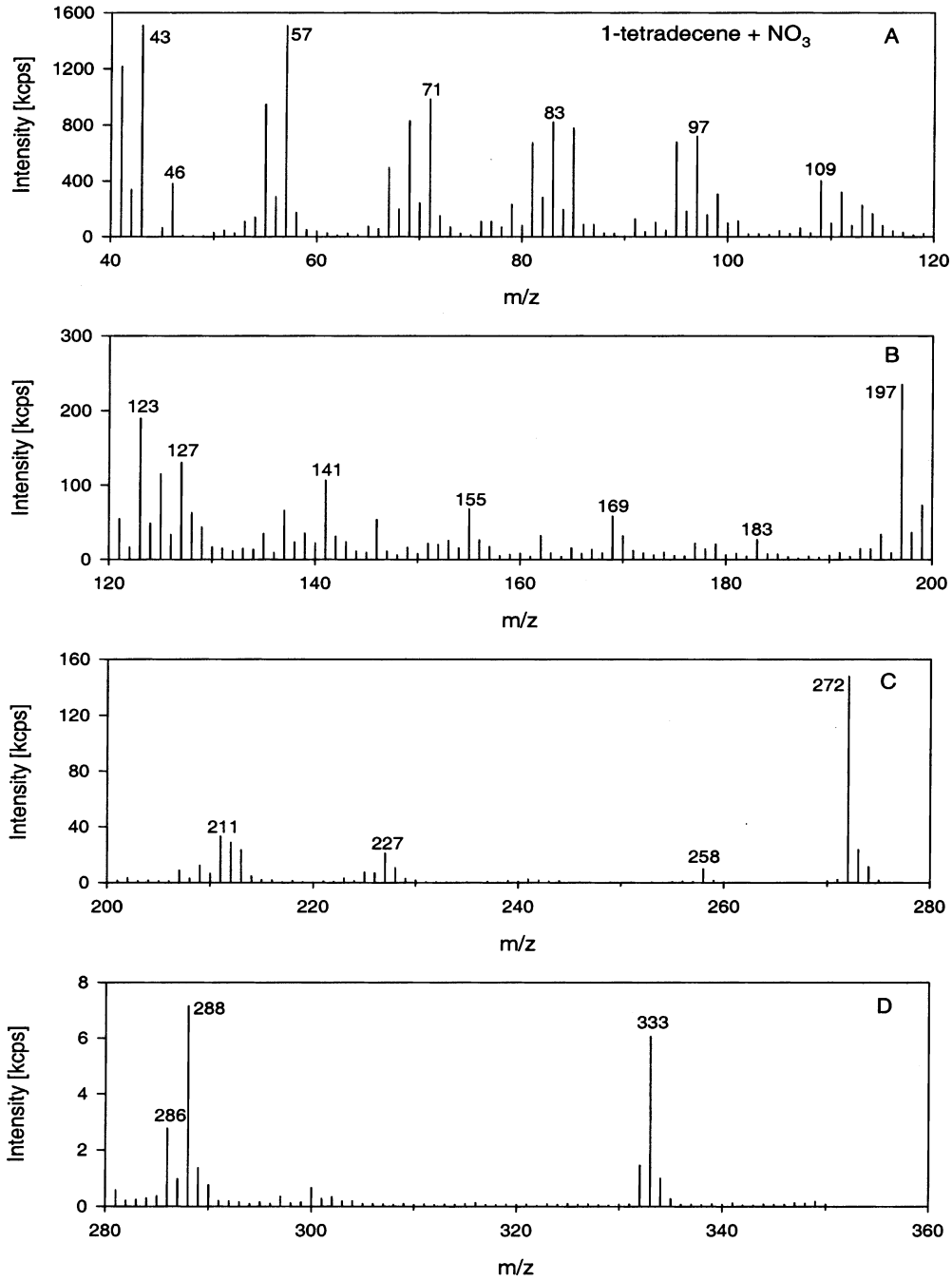

Figure 3. Real-time mass spectrum of aerosol formed in the reaction of 1-tetradecene with NO_3 radicals.

always contain a large peak at *m*/*z* $M - 33$ (*M* is the molecular ion mass) due to the loss of HO_2.[6,41] This should result in a maximum in the *m*/*z* 258 profile at 30 °C, which is absent (Figure 4D).

Among the gas-phase products that have been observed in previous studies, compounds **1**, **3**, and **4** remain as possibilities and our results suggest that the maxima at 30 and 39 °C are due to a combination of these three compounds. The assignment of compound **3**, a hydroxynitrate, as a contributor to the 30 °C compound(s) is consistent with the maximum in the *m*/*z* 199 profile shown in Figure 4B. Although mass spectra are not available for any of the proposed products, EI mass spectra are available for related compounds. For example, the mass spectrum of a 1,2-dihydroxytetradecane [$CH_3(CH_2)_{11}CH(OH)$-CH_2OH] standard, which has a similar structure to compound **3**, is shown in Figure 1S (Supporting Information). The highest mass peak is a large one at *m*/*z* 199 corresponding to the $CH_3(CH_2)_{11}CHOH^+$ ion formed by loss of $^{\bullet}CH_2OH$. Formation of this ion should be even more favored for compound **3** because of the greater stability of the HCHO and NO_2 molecules lost during decomposition (Figure 5) as compared to a $^{\bullet}CH_2OH$ radical. As expected, *m*/*z* 125 and some of the other ions in the $C_nH_{2n-1}^+$ series that is prominent in the 1,2-dihydroxytetradecane mass spectrum also exhibit maxima at 30 °C.

It appears that a second compound also desorbs at 30 °C. In the *m*/*z* 197 profile (Figure 4B), there is a shoulder at 30 °C and a peak at 39 °C. It is unlikely that the mass spectrum of compound **3** would have such an intense peak (~2−3 times larger than *m*/*z* 199) at this mass. We therefore assign this fragment to another compound with essentially the same volatility. The best candidate is compound **4**, a carbonylnitrate. It is reasonable that the volatility of this compound would be similar to compound **3**, because they only differ by carbonyl and hydroxyl groups. The large peak at *m*/*z* 197 is expected for

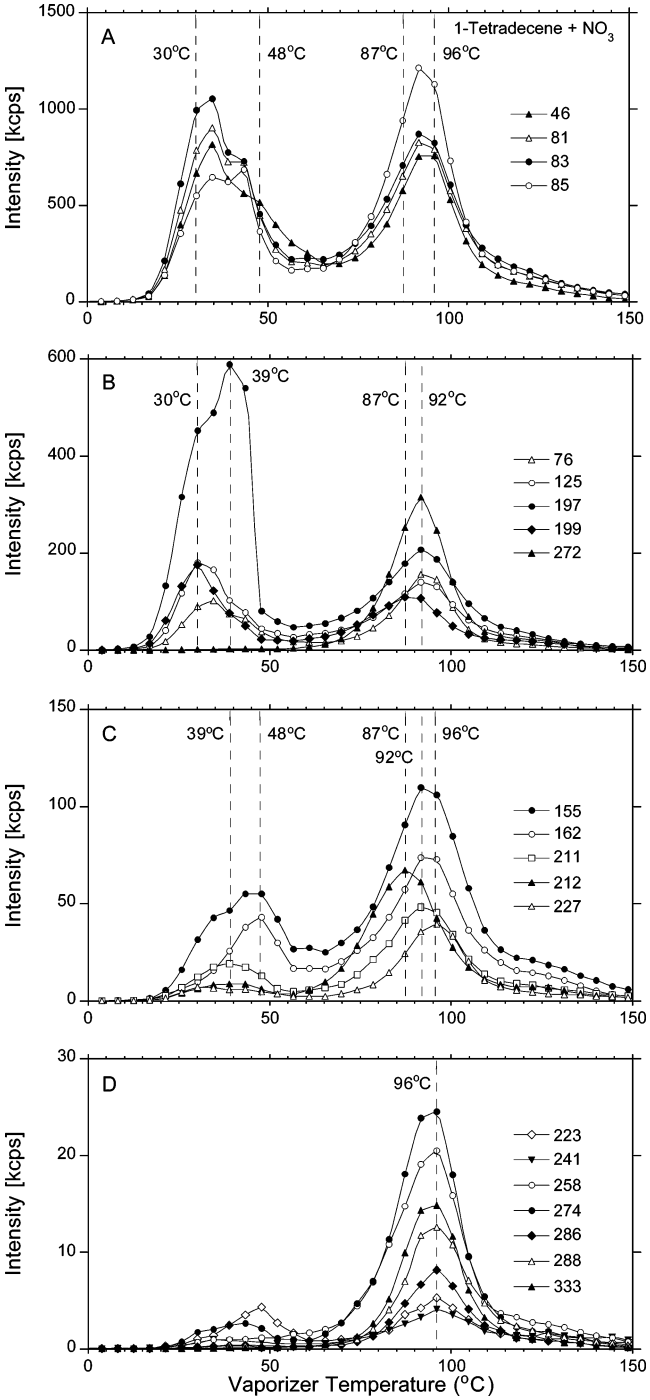

Figure 4. Thermal desorption profiles for selected *m*/*z* values for aerosol formed in the reaction of 1-tetradecene with NO_3 radicals.

compound **4**, due to the stable acylium ion, $CH_3(CH_2)_{11}CO^+$, formed by loss of HCHO and NO_2 (Figure 5). For comparison, the mass spectrum of a 2-oxoadipic acid [$HO(O)C(CH_2)_3C(O)C(O)OH$] standard shown in Figure 1S (Supporting Information) has an intense high-mass peak at *m*/*z* 115 from the acylium ion $HO(O)C(CH_2)_3CO^+$ formed by loss of the $^{\bullet}C(O)OH$ radical.

This assignment of compounds **3** and **4** is also consistent with the mass spectra of the alkyl nitrate standards ($M = 147$) shown in Figure 1S (Supporting Information). The 1-nitrooxyhexane [$CH_3(CH_2)_4CH_2ONO_2$] standard has a terminal nitrooxy group, as do compounds **3** and **4**. Bond scission at the nitrooxy carbon, which is the pathway proposed for compounds **3** and **4**, leads to *m*/*z* 71 [$CH_3(CH_2)_4^+$] or 76 [$CH_2ONO_2^+$] for 1-nitrooxyhexane and *m*/*z* 57 [$CH_3(CH_2)_3^+$] or 90 [$CH_3CHONO_2^+$] for 2-nitrooxyhexane [$CH_3(CH_2)_3CH(ONO_2)CH_3$], depending on which fragment retains the charge. The *m*/*z* 85 ion observed for both standards is due to loss of NO_3. This is not a major fragmentation pathway for compounds **3** and **4**, but is important for some second-generation products discussed below.

The maximum at 39 °C is most likely due to compound(s) **1** and/or **10**. Compound **1** is a nitrooxy peroxynitrate and compound **10** is a dihydroxy nitrate. Both should be less volatile than **3** and **4**, and can easily produce *m*/*z* 197 ions (Figure 5). It is worth noting that the similar $R-CH_2ONO_2$ structures of compounds **1**, **3**, **4**, and **10** should lead to $CH_2ONO_2^+$ ions in the mass spectra of all four compounds. The *m*/*z* 76 desorption profile shown in Figure 4B exhibits a maximum between 30 and 39 °C, indicating that all these compounds fragment by this pathway.

The compound that desorbs at 48 °C is assigned as compound **8**, a nitrooxyhydroxyalkyl peroxynitrate. If this compound fragments by pathways similar to compound **1**, the major ions contributing to the mass spectrum should be acylium ions corresponding to *m*/*z* 155 and 162 (Figure 5). The desorption profiles of both these ions exhibit maxima at 48 °C.

The next maximum observed in any desorption profile is at 87 °C, followed by maxima at 92 and 96 °C. The large temperature gap between these three maxima and those at 30, 39, and 48 °C is indicative of a significant reduction in compound vapor pressures. The much higher masses of many of the fragment ions in the mass spectra associated with the lower volatility compounds indicate they have significantly different molecular structures. In the process of analyzing these data, it became obvious that the mass spectra could not be explained on the basis of first-generation products similar to those observed in previous gas-phase studies. For example, only two first-generation products, compounds **1** ($M = 336$) and **8** ($M = 352$), have $M \geq 333$, as is necessary to produce a mass spectral peak at *m*/*z* 333. Neither of these compounds can be responsible for this peak, however, because no plausible fragmentation pathways can lead to a loss of 3 or 19 mass units. The low volatilities and high molecular weights of the products indicated that reactions were occurring that allowed a second nitrate group to be added to the molecule, because a large number of carbonyl and/or hydroxyl groups would be needed to achieve a similar effect. It appeared, therefore, that new double bonds were being formed during the reaction that allowed further addition of NO_3 radicals. This led us to the work of Martin et al.,[36] who showed that δ-hydroxycarbonyls undergo isomerization−dehydration reactions that lead to unsaturated dihydrofuran products. The rapid reaction of the dihydrofurans with NO_3 radicals would quickly form much lower volatility compounds. We therefore propose that the compounds that desorb at 87, 92, and 96 °C correspond to second-generation products consisting of hydroxy [**22**, **23**, **30**, **31**] and oxo [**24**, **32**] dinitrooxytetrahydrofurans formed by the mechanism shown in Figure 2.

All the major high-mass peaks in the mass spectrum, as well as some less prominent peaks, can be explained as stable ions formed from hydroxy and oxo dinitrooxytetrahydrofurans by loss of the molecular species H_2O, NO_2, HNO_2, NO_3, HNO_3, HCHO, $CH_2{=}CH_2$, and CO, and OH and alkyl radicals, as shown in Figure 5. For these compounds, major fragmentation pathways leading to high-mass ions are those involving the loss of substituents from the 2 and 5 positions on the ring (i.e., the two carbon atoms adjacent to the O-atom). This is demonstrated in the mass spectrum of 2-hydroxytetrahydrofuran shown in Figure 2S (Supporting Information), where loss of OH leads to

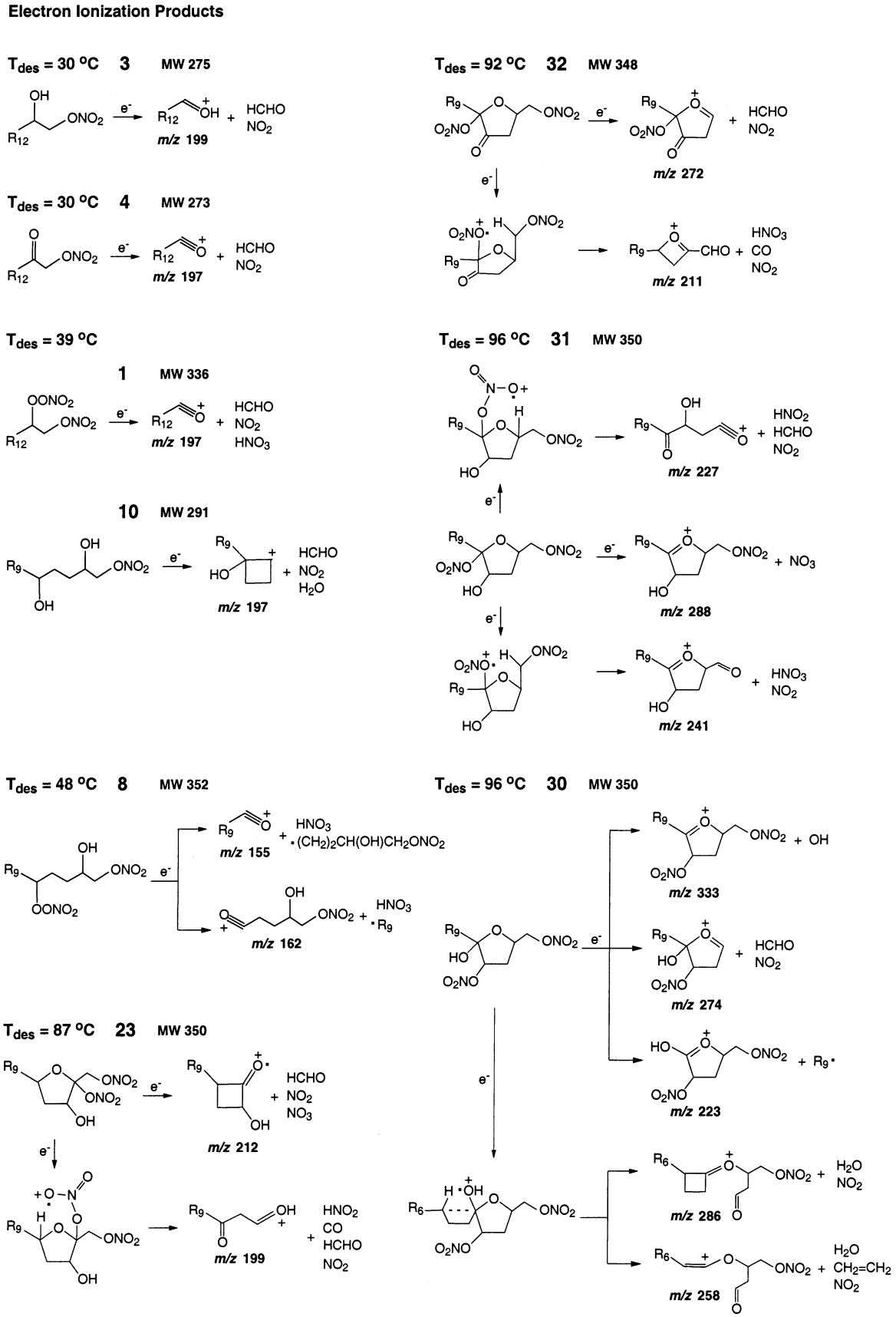

Figure 5. Proposed aerosol products for the reaction of 1-tetradecene with NO_3 radicals and electron ionization fragmentation pathways. In this figure, $R_{12} = CH_3(CH_2)_{11}$, $R_9 = CH_3(CH_2)_8$, and $R_6 = CH_3(CH_2)_5$.

the large peak at *m*/*z* 71. The *m*/*z* 333, 288, 274, 272, and 223 peaks from the 1-tetradecene reaction can all be explained by this mechanism. Functional groups in the 3 or 4 positions on the ring are apparently not lost directly, as indicated by the absence of a *m*/*z* 71 peak in the mass spectrum of 3-hydroxytetrahydrofuran shown in Figure 2S (Supporting Information).

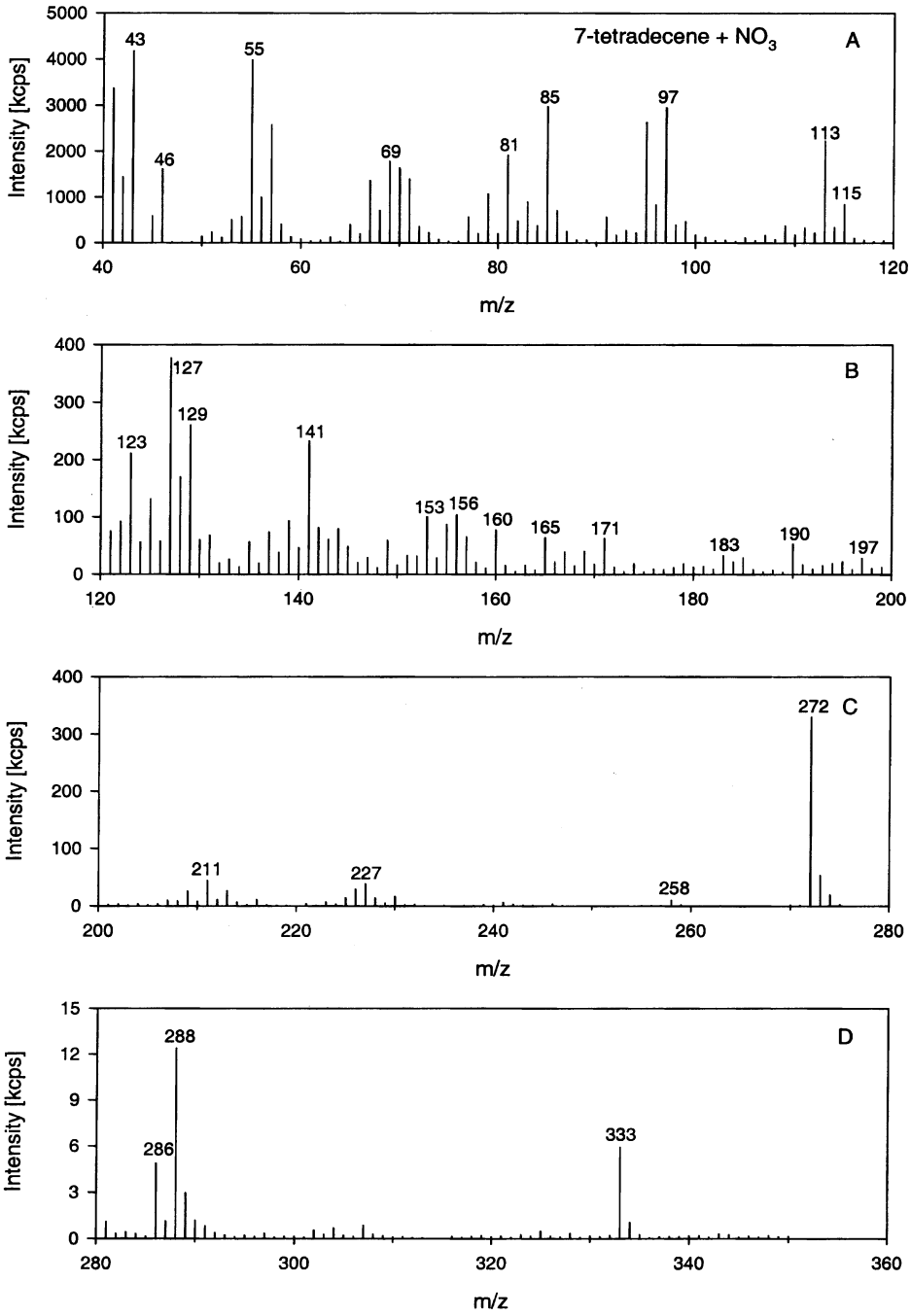

Figure 6. Real-time mass spectrum of aerosol formed in the reaction of 7-tetradecene with NO_3 radicals.

This indicates that the peaks at *m*/*z* 333 and 288, for example, are derived from different isomers having similar volatilities (Figure 5). The other major fragmentation pathways are initiated by H-atom abstraction enhanced by the formation of a six-member ring (seven-member in the case of *m*/*z* 227) transition state, which is a well-established mechanism.[40] This leads to the loss of H_2O (*m*/*z* 286 and 258), HNO_3 (*m*/*z* 241 and 211), and HNO_2 (*m*/*z* 227 and 199) followed by other stable molecules such as $CH_2{=}CH_2$, CO, HCHO, and NO_2. As shown below, the absence of a peak corresponding to *m*/*z* 286 for the reaction products of $C_n \leq 8$ alkenes is consistent with this pathway. It is important to note that although mass spectra of the hydroperoxy dinitrooxytetrahydofurans **19**, **20**, **27**, and **28** ($M = 366$) would also probably have significant peaks at *m*/*z* 333 due to loss of HO_2, the other observed ions are not consistent with fragmentation of these compounds. The second-generation products identified here have not been observed previously.

7-Tetradecene. The linear alkene 7-tetradecene [$CH_3(CH_2)_5$-$CH{=}CH(CH_2)_5CH_3$] is an isomer of 1-tetradecene with the double bond in the middle of the molecule. In this case, $R_X = CH_3(CH_2)_2$ and $R_Y = CH_3(CH_2)_5$ in Figures 1 and 2. As shown in Figure 6, this change in structure has only a minor effect on the real-time mass spectrum of the aerosol products. The same high-mass peaks are present at *m*/*z* 333, 288, 286, 274, 272, 258, 227, and 211. The peaks at *m*/*z* 199 and 197 are much reduced because of the change in length of the carbon chain adjacent to the double bond, and a few important new peaks appear, at *m*/*z* 160 and 190. The desorption profiles for selected *m*/*z* values are shown in Figure 7, and again indicate the presence of two groups of compounds: a more volatile group

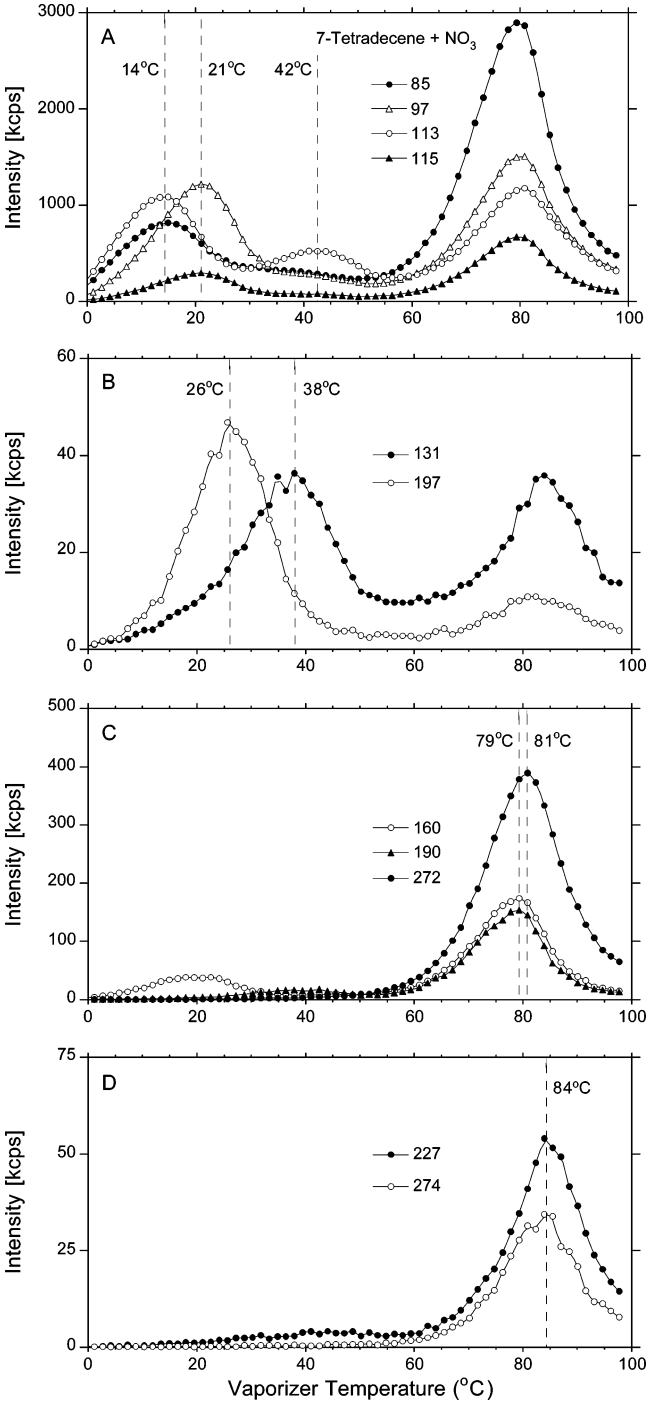

Figure 7. Thermal desorption profiles for selected *m*/*z* values for aerosol formed in the reaction of 7-tetradecene with NO_3 radicals.

(first-generation products) with maxima between 14 and 42 °C, and a less volatile group (second-generation products) with maxima between 79 and 84 °C. The fragmentation pathways proposed to be responsible for the major mass spectral peaks are shown in Figure 8 and are similar to those proposed for the 1-tetradecene reaction products.

The two most volatile aerosol products desorb at 14 and 21 °C. As with 1-tetradecene, they are assigned to compounds **3** and **4**. These compounds are more volatile than the corresponding 1-tetradecene products and also differ slightly in volatility with respect to each other. These differences are because of the shift of the functional groups from the end of the molecule to the center. The desorption profiles of *m*/*z* 85 and 113, which are indicative of a carbonylnitrate, both have maxima at 14 °C, whereas the profiles of *m*/*z* 97 and 115, which are indicative of a hydroxynitrate, both have maxima at 21 °C. The desorption profile of *m*/*z* 160 has a broad maximum spanning the region from 14 to 21 °C, indicating that this fragment comes from both compounds. The *m*/*z* 113, 115, and 160 peaks are analogous to the *m*/*z* 197, 199, and 76 peaks, respectively, observed in the 1-tetradecene reaction mass spectrum. Further fragmentation of the *m*/*z* 113 and 115 ions yield large peaks at *m*/*z* 85 and *m*/*z* 97 by loss of CO and H_2O, respectively. These pathways were not observed for the *m*/*z* 197 and 199 ions from the 1-tetradecene reaction products because of the greater stability of larger $RCHOH^+$ and RCO^+ ions. This size effect is demonstrated in the mass spectra of 5-hydroxytetradecane $[CH_3(CH_2)_3CH(OH)(CH_2)_8CH_3]$ and 7-hydroxytetradecane $[CH_3(CH_2)_5CH(OH)(CH_2)_6CH_3]$ shown in Figure 3S (Supporting Information). The $CH_3(CH_2)_8CHOH^+$ *m*/*z* 157 ion from 5-hydroxytetradecane does not lose H_2O to give a peak at *m*/*z* 139, whereas for 7-hydroxytetradecane the loss of H_2O from the smaller $CH_3(CH_2)_5CHOH^+$ and $CH_3(CH_2)_6CHOH^+$ ions is indicated by the peaks at *m*/*z* 115 and 97 and at *m*/*z* 129 and 111, respectively.

There are also maxima at 26, 38, and 42 °C in the desorption profiles of *m*/*z* 197, 131, and 113, respectively. On the basis of volatility and probable fragmentation pathways (Figure 8), the maxima at 38 and 42 °C are assigned to compounds **10** and **1**, respectively, but no plausible assignment could be made to the 26 °C maximum.

The compounds that exhibit desorption maxima between 79 and 84 °C are assigned to second-generation products, similar to the products of the 1-tetradecene reaction. Some of the desorption profiles are broader and less well resolved, but the oxo [**32** and/or **24**] and hydroxy [**30**, **31** and/or **22, 23**] dinitrooxytetrahydrofurans still desorb at slightly different temperatures. This is demonstrated in Figure 7C,D for some of the most intense high-mass fragments. It is worth noting that to form the *m*/*z* 272 and 274 ions by loss of HCHO and NO_2, an H-atom and alkyl group must exchange positions on the ring. This was unnecessary for the 1-tetradecene reaction products and suggests a strong propensity for the formation of these ions. One other difference is that for the 7-tetradecene reaction the *m*/*z* 286 ion is apparently formed from compound **22** rather than **30**, because the alkyl group must be sufficiently large for isomerization. Last, one very important observation that provides strong support for the identification of hydroxy dinitrooxytetrahydrofurans is that the *m*/*z* 160 and 190 desorption profiles both have maxima at 79 °C. These are new fragments that appear because of the different position of the double bond in 7-tetradecene. They are formed when compound **30** (and/or **31**), which has a molecular weight of 350, splits into fragments with mass 160 and 190.

The proposed first- and second-generation SOA products from the reactions of 1-tetradecene and 7-tetradecene are summarized in Table 1S (Supporting Information) along with desorption temperatures (T_{des}) and vapor pressures at 25 °C (P_{25}). The P_{25} values were estimated from T_{des} values using an empirical correlation [$\log P_{25}(\text{Pa}) = -0.0854T_{des}(°\text{C}) - 1.792$] obtained from vapor pressures of a series of $C_{13}-C_{22}$ monocarboxylic acids[42] measured using the TPTD technique.[43] These values are probably accurate to within about 1 order of magnitude.

Homologous Linear Alkenes. The mass spectral patterns observed for the aerosol products from reactions of other linear alkenes are consistent with those from 1-tetradecene and 7-tetradecene. The real-time mass spectrum of aerosol from the reaction of 1-heptene $[CH_3(CH_2)_4CH{=}CH_2]$, which was the smallest alkene to form aerosol, is shown in Figure 9. For this

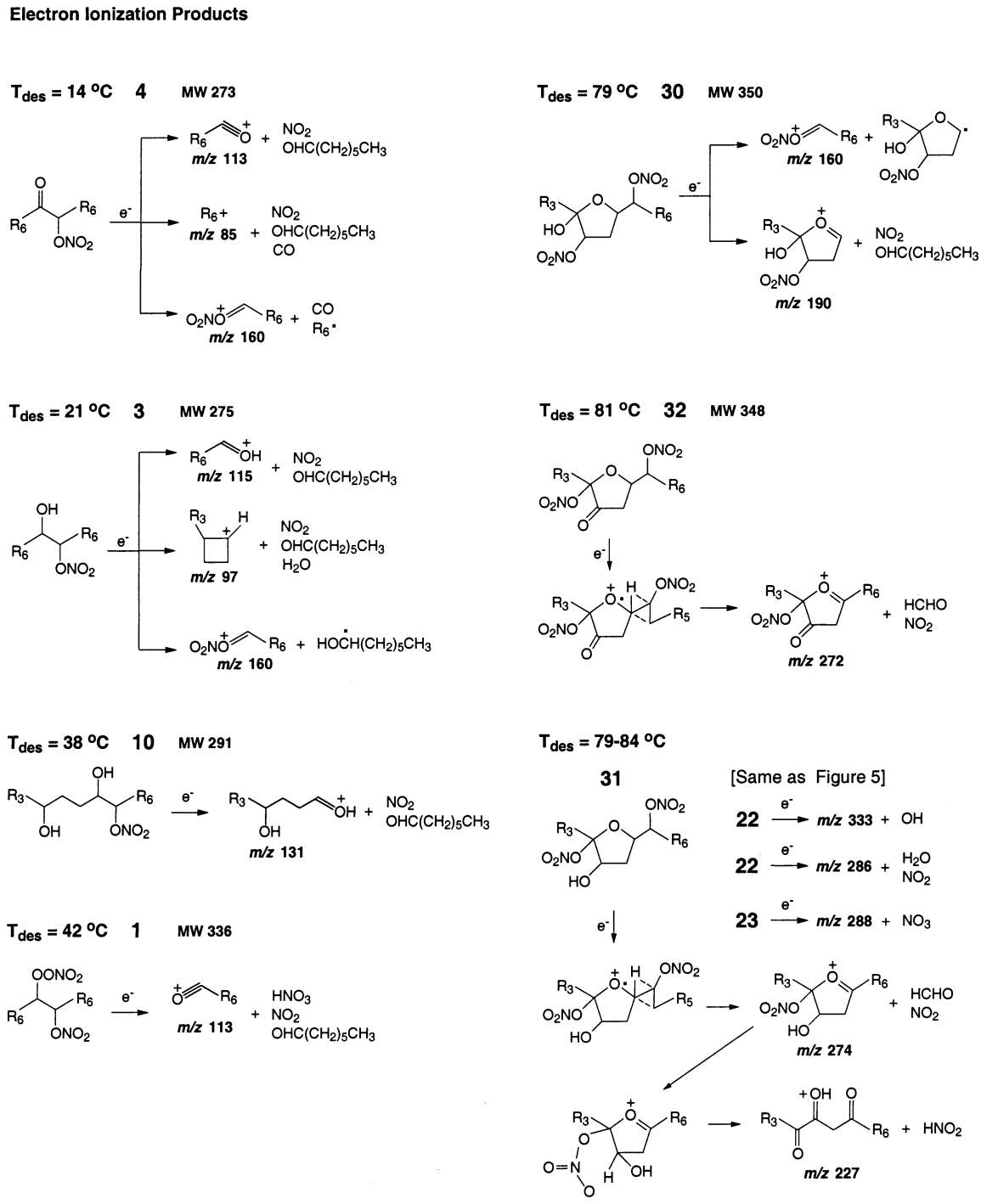

Figure 8. Proposed aerosol products for the reaction of 7-tetradecene with NO_3 radicals and electron ionization fragmentation pathways. In this figure, $R_6 = CH_3(CH_2)_5$, $R_5 = CH_3(CH_2)_4$, and $R_3 = CH_3(CH_2)_2$.

alkene, $R_X = CH_3CH_2$ and $R_Y = H$ in Figures 1 and 2. The molecular weight of 1-heptene is 98 compared to 196 for 1-tetradecene, so corresponding peaks in the mass spectra differ by 98 mass units. As expected, major high-mass peaks in the 1-heptene reaction mass spectrum are present at *m*/*z* 235, 190, and 174, corresponding to *m*/*z* 333, 288, and 272 for the 1-tetradecene reaction. No peak is present at *m*/*z* 188, which corresponds to *m*/*z* 286. This is apparently because the pathway for forming the *m*/*z* 286 ion, as proposed in Figure 5, is not accessible to the 1-heptene reaction product. This pathway involves a six-member ring transition state, and so requires a terminal alkene having at least 8 carbons. We observed peaks indicative of this pathway in the mass spectra from reactions of 1-tetradecene, 1-dodecene and 1-decene, but not 1-octene and 1-heptene. The absence of a peak for 1-octene, even though it has 8 carbons, is probably because abstraction would occur at a primary hydrogen. This requires more energy than for the secondary hydrogens available in terminal alkenes having 9 or more carbons.

Contributions of First- and Second-Generation Reaction Products to SOA Formation. Thermal desorption profiles of single *m*/*z* values are valuable for identifying products but do not provide quantitative information. Profiles of the total ion signal, however, can be used for this purpose. Because the total ion signal is approximately proportional to the organic mass,[44] the mass fraction of a component can be estimated from the normalized area under its desorption peak. This is equivalent to using a total ion chromatogram to estimate compound

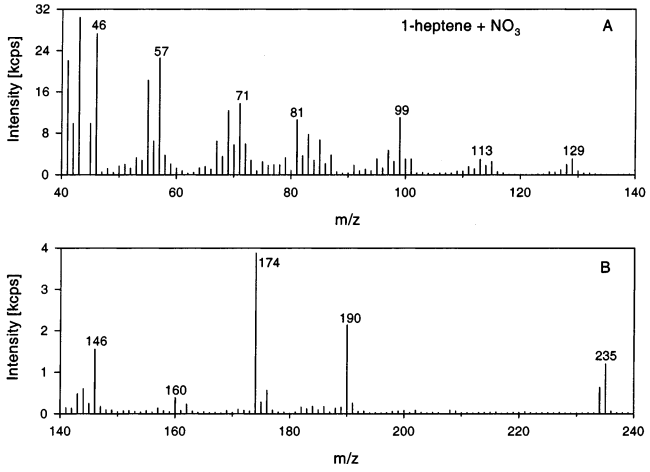

Figure 9. Real-time mass spectrum of aerosol formed in the reaction of 1-heptene with NO_3 radicals.

concentrations in GC−MS analysis. The approach is demonstrated in Figure 10 for aerosol formed from reactions of the homologous series of terminal alkenes: 1-tetradecene, 1-dodecene, 1-decene, and 1-octene.

In most cases, single compounds cannot be resolved in the plots of total ion signal, and peaks instead represent a group of compounds with similar volatilities. For example, peaks are observed at 34, 46, and 92 °C in the profile for 1-tetradecene (Figure 10A). Comparing with profiles for single *m*/*z* values (Figure 4) indicates the peak at 34 °C is from compounds that desorb at 30 and 39 °C, whereas the peak at 46 °C is from the compounds that desorb at 39 and 48 °C. The peak at 92 °C is from second-generation products that desorb between 87 and 96 °C. The interpretation of the profiles for other compounds is similar. As expected, product volatility increases as the molecular weight of the parent alkene decreases. For 1-tetradecene, 1-dodecene, 1-decene, and 1-octene, the mean desorption temperatures are 92, 81, 61, and 47 °C for second-generation products and 40, 29, and 20 for first-generation products (no 1-octene peak).

Although the resolution is not sufficient to quantify single compounds, it is possible to use these results to estimate the relative contributions of first- and second-generation products to the aerosol yield. On the basis of the discussion above, we can assume that the dividing line between first- and second-generation products in 1-tetradecene aerosol is the minimum in the curve at ∼63 °C (Figure 10A). We then use the normalized signal below and above this temperature to calculate the fraction of aerosol mass from the two components. We do the same for the other profiles using temperatures of 55 and 35 °C for 1-dodecene and 1-decene, respectively, whereas 1-octene has only second-generation products. The results of this analysis indicate that the mass fractions of first- and second-generation products are approximately 50:50, 30:70, 10:90, and 0:100, for 1-tetradecene, 1-dodecene, 1-decene, and 1-octene aerosol, respectively.

An Additional Test of the Proposed Reaction Mechanism. As shown in Figure 2, the proposed mechanism for forming second-generation reaction products requires the presence of δ-hydroxycarbonyls, which isomerize and dehydrate to form unsaturated compounds that then react with NO_3 radicals. A key step in the formation of δ-hydroxycarbonyls is a 1,5 H-atom shift within the alkoxy radical intermediate. For all the terminal alkenes discussed above, this isomerization pathway is available to the β-alkoxy radicals formed after addition of NO_3 at the terminal carbon and leads to δ-hydroxycarbonyl nitrate products

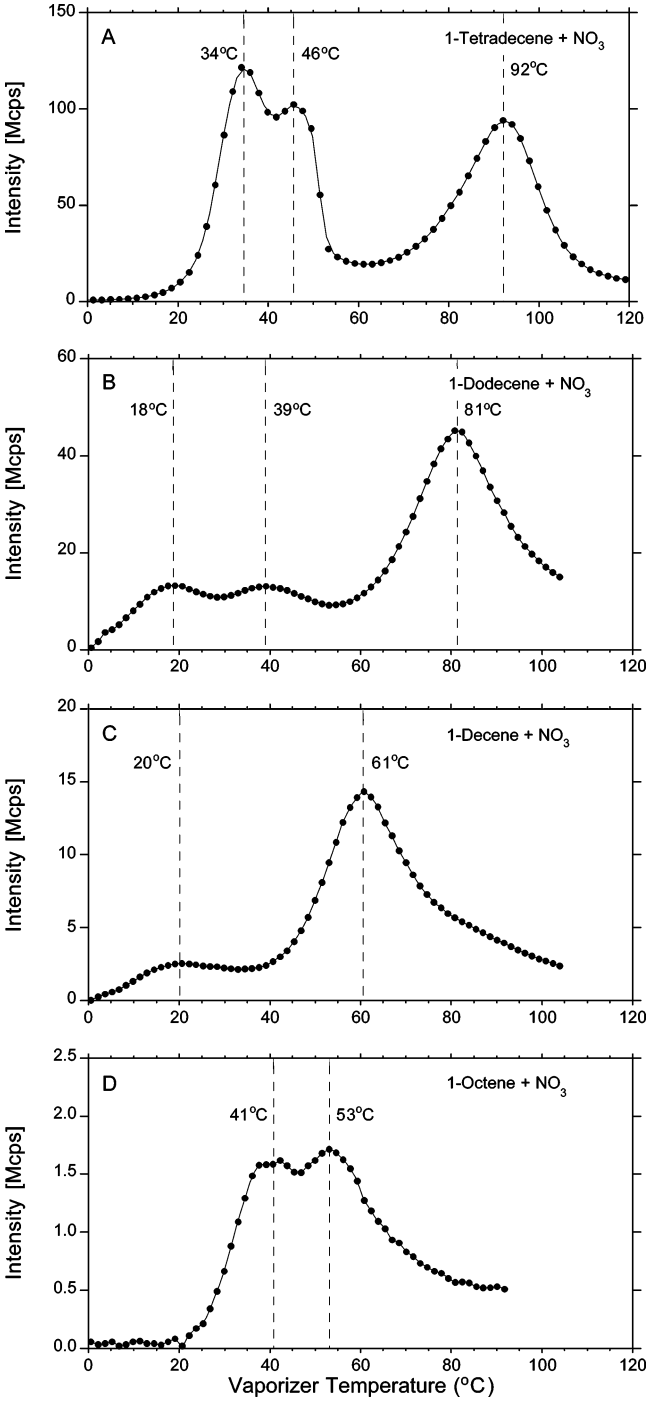

Figure 10. Total ion desorption profiles from TPTD analysis of aerosol formed in the reactions of (A) 1-tetradecene, (B) 1-dodecene, (C) 1-decene, and (D) 1-octene with NO_3 radicals.

11 and **12**. Terminal alkenes without H-atoms on the 5-carbon cannot form δ-hydroxycarbonyls or second-generation reaction products.

One terminal alkene that has no H-atoms on the 5-carbon is 3,5,5-trimethyl-1-hexene [$CH_3C(CH_3)_2CH_2CH(CH_3)CH{=}CH_2$], which is commercially available. As a test of the proposed mechanism, this compound was reacted with N_2O_5. A reaction was also performed using 2-methyl-1-octene [$CH_3(CH_2)_5C(CH_3){=}CH_2$], which is an isomer of 3,5,5-trimethyl-1-hexene that can form second-generation products. From the discussion above regarding the desorption profiles in Figure 10, aerosol formed from C_9 alkenes is composed almost entirely of second-generation products. One would therefore expect that if the

mechanism proposed here is correct, the aerosol yield from the reaction of 3,5,5-trimethyl-1-hexene should be very small and much less than that from 2-methyl-1-octene. Reactions were carried out with 1 ppmv 3,5,5-trimethyl-1-hexene and 10 ppmv N_2O_5, and 1 ppmv 2-methyl-1-octene and 2 ppmv N_2O_5. Under these conditions, reactions of both alkenes are calculated to be >90% complete within 30 min, as was verified by GC analysis of the amount of reacted alkene. The results of the experiments were consistent with the predictions of the reaction mechanism: the aerosol yield from 2-methyl-1-octene was 10%, whereas no aerosol was formed from 3,5,5-trimethyl-1-hexene.

Conclusions

The results of this study show that SOA formation from reactions of NO_3 radicals with linear alkenes involves both first- and second-generation products. The most important first-generation aerosol products are hydroxynitrates, carbonylnitrates, nitrooxyperoxy nitrates, and dihydroxynitrates. Although δ-hydroxycarbonyls are too volatile to form SOA directly, they are key intermediates in the formation of lower volatility second-generation products. Because of the 1,4 configuration of the hydroxyl and carbonyl groups in δ-hydroxycarbonyls, these compounds can readily isomerize to cyclic hemiacetals and then dehydrate to form substituted dihydrofurans. The double bonds in dihydrofurans are extremely reactive toward NO_3 radicals, so these compounds are rapidly converted to lower volatility hydroxy and oxo dinitrooxytetrahydrofurans. It is not known if the isomerization of δ-hydroxycarbonyls to cyclic hemiacetals occurs in the gas phase or requires a surface (particles or walls), but our previous studies indicated that hydroperoxycarbonyls can isomerize in the gas phase.[41]

For the C_6-C_{14} alkenes studied here at concentrations of 1 ppmv, SOA formed only for alkenes C_7 or larger. The SOA formed from reactions of C_7-C_9 alkenes consisted solely of second-generation products. First-generation products first appeared in SOA from C_{10} alkenes, and their contribution to the aerosol mass increased with increasing carbon number. In the case of 1-tetradecene, the largest alkene studied, the mass fractions of first- and second-generation products in the aerosol were ~50:50. These results are indicative of enhanced gas-to-particle partitioning for the lower volatility products formed from larger alkenes.

The important role observed here for δ-hydroxycarbonyls (through conversion to dihydrofurans) in SOA formation is likely to be of general applicability because δ-hydroxycarbonyls are also formed from reactions of hydrocarbons with OH radicals and O_3. In the atmosphere, dihydrofurans should react primarily with O_3 and NO_3 radicals,[36] which indicates that the importance of these oxidants in SOA formation is not limited to reactions of unsaturated hydrocarbons. These reactions open efficient pathways for forming low-volatility products, which are not currently included in models of SOA chemistry. Elsewhere we will demonstrate the importance of δ-hydroxycarbonyls in SOA formation from reactions of alkanes with OH radicals in the presence of NO_x.[45]

Acknowledgment. This material is based upon work supported by the National Science Foundation under Grants ATM-9816610, ATM-0234586, and ATM-0328718. Any opinions, findings, and conclusions or recommendations expressed in this material are those of the author and do not necessarily reflect the views of the National Science Foundation (NSF). We also thank Dr. Roger Atkinson and Dr. Janet Arey for helpful discussions.

Supporting Information Available: Electron ionization mass spectra of standard compounds from the Wiley Mass Spectral Database: 1-nitrooxyhexane, 2-nitrooxyhexane, 1,2-dihydroxytetradecane, 2-hydroxytetrahydrofuran, 3-hydroxytetrahydrofuran, 5-hydroxytetradecane, and 7-hydroxytetradecane; a TDPBMS mass spectrum of 2-oxoadipic acid; and a summary of the proposed first- and second-generation SOA products from the reactions of 1-tetradecene and 7-tetradecene, their desorption temperatures and estimated vapor pressures at 25 °C. This material is available free of charge via the Internet at http://pubs.acs.org.

References and Notes

(1) Seinfeld. J. H.; Pandis, S. N. *Atmospheric Chemistry and Physics*; John Wiley & Sons: New York, 1998.
(2) Atkinson R. *Atmos. Environ.* **2000**, *34*, 2063−2101.
(3) Jang, M.; Kamens, R. M. *Environ. Sci. Technol.* **2001**, *35*, 3626−3639.
(4) Larsen, B. R.; Di Bella, D.; Glasius, M.; Winterhalter, R.; Jensen, N. R.; Hjorth, J. *J. Atmos. Chem.* **2001**, *38*, 231−276.
(5) Yu, J.; Cocker, D. R.; Griffin, R. J.; Flagan, R. C.; Seinfeld, J. H. *J. Atmos. Chem.* **1999**, *34*, 207−258.
(6) Tobias, H. J.; Ziemann, P. J. *Environ. Sci. Technol.* **2000**, *34*, 2105−2115.
(7) Orlando, J. J.; Tyndall, G. S.; Moortgat, G. K.; Calvert, J. G. *J. Phys. Chem.* **1993**, *97*, 10996−11000.
(8) Atkinson, R. *J. Phys. Chem. Ref. Data* **1991**, *20*, 459−507.
(9) Wayne, R. P.; Barnes, I.; Biggs, P.; Burrows, J. P.; Canosa-Mas, C. E.; Hjorth, J.; Le Bras, G.; Moortgat, G. K.; Perner, D.; Poulet, G.; Restelli, G.; Sidebottom, H. *Atmos. Environ.* **1991**, *25A*, 1−206.
(10) Geyer, A.; Alicke, B.; Konrad, S.; Schimitz, T.; Stutz, J.; Platt, U. *J. Geophys. Res.* **2001**, *106*, 8013−8025.
(11) Geyer, A.; Alicke, B.; Ackermann, R.; Martinez, M.; Harder, H.; Brune, W.; di Carlo, P.; Williams, E.; Jobson, T.; Hall, S.; Shetter, R.; Stutz, J. *J. Geophys. Res.* **2003**, *108*, 4368−4378.
(12) Nazaroff, W. W.; Weschler, C. J. *Atmos. Environ.* **2004**, *38*, 2841−2865.
(13) Atkinson, R. *J. Phys. Chem. Ref. Data* **1997**, *26*, 215−290.
(14) Calvert, J. G.; Atkinson, R.; Kerr, J. A.; Madronich, S.; Moortgat, G. K.; Wallington, T. J.; Yarwood, G. *The Mechanisms of Atmospheric Oxidation of the Alkenes*; Oxford University Press: New York, 2000.
(15) Hallquist, M.; Wängberg, I.; Ljungström, E.; Barnes, I.; Becker, K. H. *Environ. Sci. Technol.* **1999**, *33*, 553−559.
(16) Griffin, R. J.; Cocker, D. R., III; Flagan, R. C.; Seinfeld, J. H. *J. Geophys. Res.* **1999**, *104*, 3555−3567.
(17) Noda, J.; Ljungström, E. *Atmos. Environ.* **2000**, *36*, 521−525.
(18) Moldanova, J.; Ljungström, E. *J. Aerosol. Sci.* **2000**, *31*, 1317−1333.
(19) Tobias, H. J.; Kooiman, P. M.; Docherty, K. S.; Ziemann, P. J. *Aerosol Sci. Technol.* **2000**, *33*, 170−190.
(20) Tobias, H. J.; Ziemann, P. J. *Anal. Chem.* **1999**, *71*, 3428−3435.
(21) Atkinson R.; Arey, J. *Chem. Rev.* **2003**, *103*, 4605−4638.
(22) Atkinson, R.; Plum, C. N.; Carter, W. P. L.; Winer, A. M.; Pitts, J. N., Jr. *J. Phys. Chem.* **1984**, *88*, 1210−1215.
(23) Finlayson-Pitts, B. J.; Pitts, J. N., Jr. *Chemistry of the Upper and Lower Atmosphere*; Academic Press: San Diego, 2000.
(24) Liu, P.; Ziemann, P. J.; Kittelson, D. B.; McMurry, P. H. *Aerosol Sci. Technol.* **1995**, *22*, 293−313.
(25) Liu, P.; Ziemann, P. J.; Kittelson, D. B.; McMurry, P. H. *Aerosol Sci. Technol.* **1995**, *22*, 314−324.
(26) Odum, J. R.; Hoffmann, T.; Bowman, F.; Collins, D.; Flagan, R. C.; Seinfeld, J. H. *Environ. Sci. Technol.* **1996**, *30*, 2580−2585.
(27) Wang, S. C.; Flagan, R. C. *Aerosol Sci. Technol.* **1990,** *13*, 230−240.
(28) Tobias, H. J.; Beving, D. E.; Ziemann, P. J.; Sakurai, H.; Zuk, M.; McMurry, P. H.; Zarling, D.; Waytulonis, R.; Kittelson, D. B. *Environ. Sci. Technol.* **2001**, *35*, 2233−2243.
(29) Jay, K.; Stieglitz, L. *Chemosphere* **1989**, *19*, 1939−1950.
(30) Barnes, L.; Bastian, V.; Becker, K. H.; Tong, Z. *J. Phys. Chem.* **1990**, *94*, 2413−2419.
(31) Skov, H.; Hjorth, J.; Lohse, C.; Jensen, N. R.; Restelli, G. *Atmos. Environ.* **1992**, *26A*, 2771−2783.
(32) Wängberg, I. *J. Atmos. Chem.* **1993**, *17*, 229−247.
(33) Kwok, E. S. C.; Aschmann, S. M.; Arey, J.; Atkinson, R. *Int. J. Chem. Kinet.* **1996**, *28*, 925−934.
(34) Tuazon, E. C.; Alvarado, A.; Aschmann, S. M.; Atkinson, R.; Arey, J. *Environ. Sci. Technol.* **1999**, *33*, 3586−3595.
(35) Cavalli, F.; Barnes, I.; Becker, K. H. *Environ. Sci. Technol.* **2000**, *34*, 4111−4116.

(36) Martin, P.; Tuazon, E. C.; Aschmann, S. M.; Arey, J.; Atkinson, R. *J. Phys. Chem. A* **2002**, *106*, 11492−11501.
(37) Reisen, F.; Aschmann, S. M.; Atkinson, R.; Arey, J. *Environ. Sci. Technol.*, in press.
(38) Baker, J.; Arey, J.; Atkinson, R., manuscript in preparation.
(39) Holt, T.; Atkinson, R.; Arey, J., manuscript in preparation.
(40) McLafferty F. W.; Turecek, F. *Interpretation of Mass Spectra*; 4th ed.; University Science Books: Sausalito, CA, 1993.
(41) Ziemann, P. J. *J. Phys. Chem. A* **2003**, *107*, 2048−2060.
(42) Chattopadhyay, S.; Ziemann, P. J. *Aerosol Sci. Technol.*, submitted for publication.
(43) Chattopadhyay, S.; Tobias, H. J.; Ziemann, P. J. *Anal. Chem.* **2001**, *73*, 3797−3803.
(44) Crable, G. F.; Coggeshall, N. D. *Anal. Chem.* **1958,** *30*, 310−313.
(45) Lim, Y. B.; Ziemann, P. J. *Environ. Sci. Technol.*, manuscript in preparation.